Turning to mechanistic questions, it is clear that only $h'_5{}^{V*V}$–$h'_8{}^{V*V}$ and their enantiomers imply net motion of the metal atom from one allene "π-bond" to the other. Mechanisms which imply these four reactions are shown in Figures 9c–f. If we assume that all intermediate configurations have connectivities equal to two, then these mechanisms imply only the reactions indicated in Figures 9c–f. Symmetry arguments do not demand that the intermediates drawn have connectivities greater than two. As noted above, however, reactions $h'_7{}^{V*V}$ and $h'_8{}^{V*V}$ must occur with equal probability. Reactions $h'_5{}^{V*V}$ and $h'_6{}^{V*V}$ need not occur with equal probability, but if ligands B_5 and C_6 have similar chemical properties, then these reactions have similar probability of occurring. Since $h'_5{}^{V*V}$–$h'_8{}^{V*V}$ are all differentiable in a totally symmetric environment, detailed nmr line shape analysis may allow distinction between "helical" movement of the allene ligand and isomerization *via* an intermediate configuration having coplanar allenyl methyl groups. Note that this final example has been simplified by assuming that rapid "π-rotation" about the metal–allene band does not occur. Should such rotation in fact occur, the distinction will be impossible.

Acknowledgments. I am grateful to Dr. Bertram Frenz for critical comments and to Mrs. Irene Casimiro for her patience in preparing the manuscript for publication.

Collisional Activation Spectra of Organic Ions[1,2]

F. W. McLafferty,* P. F. Bente, III, Richard Kornfeld, Shih-Chuan Tsai, and Ian Howe[2c]

Contribution from the Department of Chemistry, Cornell University, Ithaca, New York 14850. *Received January 20, 1972*

Abstract: Collision with neutral molecules is shown to provide a convenient method of adding internal energy to ions in a field-free drift region of the mass spectrometer. The effects on this process of ion accelerating potential, target gas pressure and identity, and precursor ion internal energy and mass have been investigated to optimize experimental conditions. Such collisions cause ion decompositions whose activation energies cover a broad range; for a particular ion such decompositions can be viewed as its "collisional activation (CA) spectrum." CA spectra, which can be obtained for each ion in the normal mass spectrum, and which appear to follow the predictions of the quasi equilibrium theory, show many more of the possible unimolecular ion decomposition reactions for an ion than do unimolecular metastables, and thus provide valuable information for ion reaction mechanisms and molecular structure determination. Collisional activation can sometimes yield ion energies which are relatively inaccessible by electron impact. The precursor ion internal energy has a negligible effect on the ion's CA spectrum except for product ions formed through the processes of lowest activation energy. Thus, CA spectra should also be valuable for the characterization of ion structures.

The dissociation of a metastable organic ion in a field-free drift region of the mass spectrometer can indicate the masses of both the precursor and daughter ions of the reaction involved. This extra dimension of information is valuable for the elucidation of reaction pathways,[3,4] and for structure determination of mixture components[3–5] and of isomeric molecules and ions.[6] Experimentally, the utility of this information has been greatly increased by the development of a defocusing technique for measuring the spectrum of daughter ions from a particular precursor with high sensitivity.[4,7] Unfortunately, for many abundant fragment ions in mass spectra the corresponding metastable ion decompositions are not found in appreciable abundance.

Ions undergoing unimolecular decomposition in the drift region ("metastables") must necessarily have lower average internal energies than those decomposing in the ion source; such metastables thus only represent the mass spectral reactions of lowest activation energy, such as rearrangements.[4,8] Such low energy reactions allow the greatest opportunity for prior isomerization ("scrambling") of the precursor ion[4,9] and can exhibit unusually high isotope effects.[10] Ion structure characterization based on metastable ion abundances[6] is compromised by their dependence on ion internal energy.[4,11]

(1) Metastable Ion Characteristics. XXII. Part XXI: D. J. McAdoo, F. W. McLafferty, and T. E. Parks, *J. Amer. Chem. Soc.*, **94**, 1601 (1972).

(2) (a) A portion of this work was reported in a preliminary communication: F. W. McLafferty and H. D. R. Schuddemage, *ibid.*, **91**, 1866 (1969). (b) Further details are given in the Cornell University Ph.D. theses of R. K., 1971, and S.-C. T., 1972. (c) Postdoctoral Fellow, 1969–1970. (d) We are grateful to the National Institutes of Health (GM 16575 and 16609) and the Army Research Office (D31-124-G1117) for generous support of this work.

(3) K. Biemann, "Mass Spectrometry, Organic Chemical Applications," McGraw-Hill, New York, N. Y., 1962, p 153; F. W. McLafferty, "Interpretation of Mass Spectra," W. A. Benjamin, New York, N. Y., 1966, p 64.

(4) For recent reviews, see K. R. Jennings, "Mass Spectrometry: Techniques and Applications," G. W. A. Milne, Ed., Wiley-Interscience, New York, N. Y., 1971, p 419; J. H. Beynon and R. M. Caprioli, "Biochemical Applications of Mass Spectrometry," G. R. Waller, Ed., Wiley-Interscience, New York, N. Y., 1972, p 157.

(5) F. W. McLafferty, R. Venkataraghavan, and P. Irving, *Biochem. Biophys. Res. Commun.*, **39**, 274 (1970).

(6) F. W. McLafferty and T. A. Bryce, *Chem. Commun.*, 1215 (1967); T. W. Shannon and F. W. McLafferty, *J. Amer. Chem. Soc.*, **88**, 5021 (1966).

(7) T. Wachs, P. F. Bente, III, and F. W. McLafferty, *Int. J. Mass Spectrom. Ion Phys.*, **9**, 333 (1972).

(8) F. W. McLafferty and R. B. Fairweather, *J. Amer. Chem. Soc.*, **90**, 5915 (1968).

(9) A. N. H. Yeo and D. H. Williams, *ibid.*, **91**, 3582 (1969).

(10) B. J.-S. Wang and E. R. Thornton, *ibid.*, **90**, 1216 (1968).

(11) J. L. Occolowitz, *ibid.*, **91**, 5202 (1969); A. N. H. Yeo and D. H. Williams, *ibid.*, **93**, 395 (1971).

Abundant ions in mass spectra can also arise from decompositions of high activation energy, for which such disadvantages are reduced. These reactions commonly involve a simple bond cleavage, so that they are more readily interpretable for structure determination. Obviously it would be desirable to be able to obtain metastable-type information about these important high energy reactions also; for this it is necessary to cause such decompositions to take place in a field-free drift region of the spectrometer. It has been recognized for many years that the collision of an ion with a neutral atom or molecule can cause ion decomposition; this was postulated to account for diffuse low-intensity peaks, often called "Aston bands," observed in early mass spectral studies.[4,12-15] For the relatively small molecules studied to date, collision-induced reactions resemble those resulting from electron impact, indicating that the collisional energy is randomized before fragmentation.[13-15] Collisional activation can add a substantial amount of energy to an ion (more than 12 eV in a particular example[15a]). Collisional activation with high energy (>1 keV) ions involves electronic excitation,[13,16] while vibrational excitation predominates only at lower ion energies.[16,17] Some decompositions may arise through collision-induced predissociation, in which a collision causes an excited ion to undergo a radiationless transition to a dissociative state of the same energy.[16] This paper extends these basic studies of collisional activation (CA) to the kinetics and mechanisms of the CA fragmentation of larger molecules, and assesses the usefulness of CA spectra in studies of molecular structure, ion structure, and ion fragmentation mechanisms.[2a,14]

Experimental Section

Most of the reported data were determined on a Hitachi RMU-7 double-focusing mass spectrometer with a "bright" ion source, Model MS-101, with ionizing electrons of 70-eV energy and 100-μA total emission, ion accelerating potential of 3.75 kV, source temperature of 180°, and slit widths of approximately 0.5 mm.

The pressure studies of Figure 5 and other data as noted were measured on a Hitachi RMH-2 double-focusing instrument operated at 70-eV electron energy, 1.2-mA total emission, source temperature of 200°, ion accelerating potential of 10.0 kV, and slit widths of 0.3 mm.[18] Ion decompositions occurring in the field-free drift region between the ion source and the electrostatic analyzer (ESA) were measured using the Barber-Elliot-Major defocusing technique.[4] In specific later experiments the RMU-7 ion source and collector were interchanged; ions separated by the magnetic sector which decompose in the following field-free region give products which can be measured by scanning the ESA.[7] The field-free collision regions have lengths of approximately 40 and 60 cm respectively in the RMU-7 and RMH-2, representing 25% of the total ion path.

The target gas (Ar or He) was introduced directly into the collision region, which is defined by the source and α slits, through a separate inlet system containing a variable leak valve. Pressures were measured with a Bayard-Alpert-type ionization gauge and corrected for collision gas identity. In the RMU-7, pressures measured on the 1.9-cm diameter collision gas inlet line and on the collision region pumping line (5-cm diameter) were linearly related and differed by a factor of 1.7. The reported pressures were obtained by multiplying the pressure measured at the pumping line by a factor of 1.2. The linear pressure plots of Figures 3, 4, and 6 indicate that the drift region pressure is linearly proportional to the measured pressure.[18] To obtain reproducible target gas pressures conveniently, the pressure is adjusted to reduce the precursor ion current to a particular fraction of the low pressure value (Figures 3, 4, and 6). A proportion of 10% appears to provide a near optimum combination of sensitivity and excitation energy for most ions. Under these conditions in general, it is possible to obtain useful CA spectra from peaks whose abundance is 0.1-1% of that of the base peak in an EI spectrum using the defocusing technique. In the RMH-2 pressures were measured on the 1.9-cm diameter collision gas inlet line approximately 30 cm from the drift region. Pressures above 3×10^{-4} Torr were corrected linearly to give linear pressure plots of the type shown in Figure 3.

A separate pumping system was added to the collision region of the RMU-7; the RMH-2 has an even more efficient multiple differential pumping system along the ion path. When the pressure in the collision region of the RMH-2 is in the 10^{-4} Torr range, the pressures in the ion source and in the ESA are about 1 and 5%, respectively, of this value; under comparable conditions in the RMU-7 the pressures in the ion source and in the second field-free drift region between the ESA and magnet are about 5 and 25%, respectively.

Consistent with this, and with the higher ion accelerating potential of the RMH-2, the maximum abundances, relative to the normal ions, of the CA spectrum from 1-propanol were found to be approximately four times as great for the RMH-2 as for the RMU-7. The only apparent effect of the collision gas on the normal performance of either instrument is a substantial broadening of the peaks at higher collision gas pressures.

Ion intensities were corrected for the variation of the response of the multiplier with the kinetic energy of the impinging ion,[19] assuming that a linear relationship exists between the kinetic energy of the ion and the multiplier response. The intensities of ions from the drift-region decomposition $m_1 \rightarrow m_2$ were accordingly multiplied by the factor $(m_1)/(m_2)$. As noted, this correction was not made for certain He data and is not necessary for most applications.

Appearance potentials, determined by Kiser's[20] energy compensation technique, were taken as the voltage at which the abundance is 0.1% of its value at 50 eV, referred to the value of benzene as 9.3 eV.

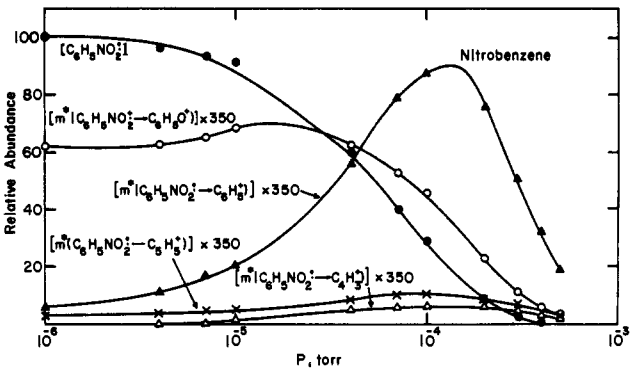

Figure 1. Unimolecular metastable and collisional activation product ion abundances as a function of pressure for molecular ions of nitrobenzene.

Results and Discussion

Similarity of Collisional Activation and Normal Mass Spectra. The effect of argon pressure in the field-free drift region on metastable ion abundances is illustrated in Figure 1.[18] Raising the pressure can cause dramatic

(12) F. W. Aston, "Mass Spectra and Isotopes," Edward Arnold, Ltd., London, 1942, pp 61-63.
(13) H. M. Rosenstock and C. E. Melton, *J. Chem. Phys.*, 26, 314, 568 (1957); C. E. Melton in "Mass Spectrometry of Organic Ions," F. W. McLafferty, Ed., Academic Press, New York, N. Y., 1963, p 102.
(14) W. F. Haddon and F. W. McLafferty, *J. Amer. Chem. Soc.*, 90, 4745 (1968); W. F. Haddon and F. W. McLafferty, *Anal. Chem.*, 41, 31, (1969).
(15) (a) K. R. Jennings, *Int. J. Mass Spectrom. Ion Phys.*, 1, 227 (1968); (b) F. Kaplan, *J. Amer. Chem. Soc.*, 90, 4483 (1968); (c) L. P. Hills, M. L. Vestal, and J. H. Futrell, *J. Chem. Phys.*, 54, 3834 (1971).
(16) H. Yamaoka, P. Dong, and J. Durup, *ibid.*, 51, 3465 (1969); C. Lifshitz, *Isr. J. Chem.*, 7, 261 (1969), and references cited therein.
(17) M. H. Cheng, M. H. Chiang, E. A. Gislason, B. H. Mahan, C. W. Tsao, and A. S. Werner, *J. Chem. Phys.*, 52, 6150 (1970); P. C. Cosby and T. F. Moran, *ibid.*, 52, 6157 (1970), and references cited therein.
(18) Further details are given in ref 2b and 7.
(19) C. La Lau, "Topics in Organic Mass Spectrometry," A. L. Burlingame, Ed., Wiley-Interscience, New York, N. Y., 1970.
(20) R. W. Kiser, "Introduction to Mass Spectrometry and Its Applications," Prentice-Hall, Englewood Cliffs, N. J., 1965.

changes in the abundances of ions so produced through competing effects; at 10^{-3} Torr essentially all of the ions are lost through scattering.

Subtraction of the unimolecular metastable ion (MI) spectrum (low pressure) from the high-pressure data gives the CA spectrum; examples are shown in Table I for activation of a variety of molecular ions. In many cases the CA spectra resemble normal electron ionization (EI) spectra, as observed previously,[13-15] supporting a general mechanism in which collision causes conversion of part of the ions' translational energy into internal energy. The resulting total internal energy of the ion should determine the probability of any subsequent ion decomposition according to the quasiequilibrium theory.

Table I. Comparison of Collisional Activation and Electron Ionization Spectra[a]

		CA spectra[d]			
m/e	AP, eV[b]	1×10^{-4} Torr	5×10^{-4} Torr	9×10^{-4} Torr	EI spectrum
		Nitrobenzene			
123[c]	9.6	4050	340	95	28
93	10.1	11 (10)[d]	5	<7	7
77	11.2	66 (67)	70	55	49
65	10.8	9	5	<8	8
51	14.4	9	13	19	25
50	16.4	5	7	11	11
		Benzonitrile			
103[c]	9.7	6460	654	210	163
76	13.3	64 (61)	53 (52)	44	49
75	15.2	12 (13)	12	10	15
51	15.7	12 (13)	14	13	13
50	15.0	12 (13)	20 (21)	33	23
		Anisole			
108[c]	8.6	5610	447	168	69
93	11.3	11	6	5	7
78	10.9	37 (36)	34 (33)	32	27
77	13.0	23	19	22	10
65	12.3	18	19	22	33
51	16.0	8	14	14	8
39	14.3	4	8	<5	15
		1-Propanol			
60[c]	10.0	1560	119	38	4
59	10.2	28 (30)	19	11	6
42	10.3	39 (35)	30 (28)	14	7
31	11.1	28 (30)	42 (43)	60	67
29	12.4	3	6	12	9
27	13.8	2	3	3	10
		2-Hexanone			
100[c]	9.2	1560	88	17	10
85	9.4	56 (53)	36 (35)	22	4
71	10.3	13 (14)	13	<5	4
58	10.0	22 (24)	25	28	25
57	11.0	1	<1	<7	10
43	11.1	8	23	33	46
29	12.7	<1	<3	<5	12
		Acetophenone			
120[c]	9.1	1680	128	39	19
105	9.6	94 (92)	77 (76)	71	47
77	12.5	6 (8)	8	11	34
51	15.7	<6	5	10	11
43	12.4	<8	9	8	7

[a] Ionization by 70-eV electrons. Ion abundances based on total fragment ion abundances = 100. [b] Appearance potential of normal ion. [c] Precursor ion in CA spectrum, molecular ion in EI spectrum. [d] Using argon as the target gas. Observed total ion abundances minus abundances of MI spectrum; for values in parentheses, the MI spectral values are corrected for the effect of ion mass on scattering.

Within experimental error the CA spectra show no appreciable change with argon pressure below approximately 1×10^{-4} Torr; at this pressure the calculated ion mean free path will be equal to the length of the metastable drift region for an ion collision diameter of 5 Å. Similarly, at 5×10^{-4} Torr after an ion has undergone an initial collision there will be approximately a 60% probability that the ion, or its decomposition product, will experience a second collision. A smaller average addition of internal energy from each collision than from 70-eV electron bombardment is indicated; similar conclusions were drawn from isotope effect studies.[21] Note that as the pressure is increased the abundance of ions of higher appearance potential (AP) increases relative to that of lower AP ions. This in part is due to preferential scattering of higher mass ions (*vide infra*); this also can be due to further collision and decomposition of primary product ions after their formation in the field-free drift region. For example, increasing pressure causes *m/e* 50 in the CA spectrum of the *m/e* 123 (molecular) ion of benzonitrile to increase at the expense of *m/e* 76; consistent with this, the CA spectrum at 1×10^{-4} Torr of the *m/e* 76 ion from benzonitrile shows *m/e* 75, 51, and 50 ions in abundances 35, 5, and 60, respectively. Note, however, that high AP reactions can result from a single collision; from the nitrobenzene molecular ion an appreciable quantity of the *m/e* 50 ion is formed at 1×10^{-4} Torr, although this requires the transfer of at least 6.3 eV of energy.

The ion kinetic energy (KE) also affects the probable amount of energy transferred (ΔE). From the Massey "adiabatic criterion," $(2\mathrm{KE}/m)^{1/2} = a\Delta E/h$[22] ($h$ is Planck's constant), an interaction limit (adiabatic parameter, a) of 10 Å predicts a most probable ΔE (for a *broad* range of values) of 0.6 eV for an ion of mass (m) 30 and 0.15 eV for one of mass 480 for an accelerating potential of 3.6 keV. In the CA spectra of the molecular ion of 1-propanol (Table II) the product ion of highest appearance potential, CH_3O^+, increases sharply with increasing ion accelerating potential; $[M\cdot^+ \rightarrow CH_3O^+]/[M^+ \rightarrow C_3H_6{}^+]$ for the Hitachi RMH-2 operating at 9.6 keV accelerating potential

Table II. Collisional Activation Spectra of 1-Propanol Molecular Ion at Various Ion Accelerating Potentials (IA)

IA, V	Ion product *m/e*	Ar pressure, Torr 1×10^{-4}	Ar pressure, Torr 5×10^{-4}
450	59	21	*a*
	42	64	*b*
	31	15	*a*
1250	59	32	28
	42	46	35
	31	23	37
3750	59	32	21
	42	38	29
	31	30	50

[a] Not detectable. [b] Barely detectable.

(21) I. Howe and F. W. McLafferty, *J. Amer. Chem. Soc.*, **93**, 99 (1971).

(22) H. S. W. Massey and E. H. S. Burhop, "Electronic and Ionic Impact Phenomena," Oxford University Press, London, 1952, p 513.

is nearly double that for the 3.75-keV data of Table II. The ion internal energy also influences the effect of increased ion accelerating potential on the cross-section for collisional excitation (Figure 2). Toluene ions with low internal energy, such as those made by ionization with 12 eV electrons, are not sufficiently excited by collision after 1.2 keV acceleration to undergo decomposition, although 2.4 and 3.6 keV acceleration does produce sufficient excitation.

In general, the size of the target gas atoms or molecules used has the expected[13,16,23] effect; using H_2 and He as target gases yields CA spectra of about twice the intensity as those using Ar. These measurements were made at the pressure of maximum absolute abundance using a variety of precursor ions.[18] We now use He generally as the target gas for analytical purposes.

Kinetics. The effect of variation in target gas pressure, [X], on the relative abundance of the precursor ion, [A], and the total daughter ions, [D], is shown by the typical examples[18] in Figures 3–6. $[A_0]$, the concentration of A ions at the entrance to the collision region, is equal to [A] + [D] at negligible target gas pressure. The linear plot of $\ln [A]/[A_0]$ *vs.* [X] shows a first-order dependence on target gas pressure. The small ratio generally found for [D]/[A] (Figures 1–3 and 5, Table I) indicates that the dominant reactions of A are those leading to ion loss, such as scattering or charge exchange; however, in certain cases [D]/[A] becomes >1 at high pressures.

Although plots of [D]/[A] *vs.* [X] show the expected linear relationship for pressures up to approximately 1×10^{-4} Torr, above this pressure many of the plots show a significant upward deviation which has not been noted previously. This behavior is found in three experimental systems of different ion path geometry and with substantial variations in internal and kinetic energy of the ions, in types of ions, and in target gases.[18] This nonlinearity apparently arises from the differences in scattering and activation cross-sections for the precursor and daughter ions, which lead to larger relative losses of the precursor ion at higher pressures, as indicated by the following kinetic treatment.

It is assumed that processes which lead to collisional activation and scattering of the precursor and daughter ions are linearly dependent on the collision gas density [X], and that unimolecular decompositions of the precursor ions are independent of [X]. D_i ($i = 1, n$)

$$A^+ \xrightarrow{k_{u_i}} D_i^+$$

$$A^+ + X \xrightarrow{k_s^A} \text{scattering loss of } A^+$$

$$A^+ + X \xrightarrow{k_{c_i}} D_i^+$$

$$D_i^+ + X \xrightarrow{k_s^{D_i}} \text{loss of } D_i^+ \text{ by scattering or further collisional activation}$$

are the various daughter ions produced by unimolecular or collision-induced decomposition. Although the scattered ions are produced with a range of momenta and angles, it is assumed that these do not change appreciably with collision gas pressure and that an average scattering cross-section, k_s, can be used. Since the velocity of the daughter ions resulting from decompositions occurring in the drift region will be equal to the velocity of the precursor ions (v_A), where $m_A v_A^2/2$ = accelerating potential, the time for the ion to travel a distance x in the drift region is given by x/v_A. Solving the $n + 1$ rate equations with the boundary conditions that [A] = $[A_0]$ and $[D_i] = 0$ at the entrance to the drift region gives the following expression for the intensity of A^+ ions leaving the drift region of length l

$$[A] = [A_0] \exp\left\{-\left(\sum_{i=1}^{n} k_u + \sum_{i=1}^{n} k_{c_i}[X] + k_s^A[X]\right) l/v_A\right\}$$

The intensity of the ith daughter ion leaving the drift region is given by eq 1 and the ratio of the two is

$$[D_i] = \frac{(k_{u_i} + k_{c_i}[X])[A_0]}{\sum_{i=1}^{n}(k_{u_i} + k_{c_i}[X] + (k_s^A - k_s^{D_i})[X]} \times \left\{\exp[-k_s^{D_i}[X]l/v_A] - \exp\left[-\sum_{i=1}^{n}(k_{u_i} + k_{c_i}[X])l/v_A - k_s^A[X]l/v_A\right]\right\} \quad (1)$$

given in eq 2. This equation is of the form given

$$\frac{[D_i]}{[A]} = \frac{k_{u_i} + k_{c_i}[X]}{\sum_{i=1}^{n}(k_u + k_{c_i}[X]) + (k_s^A - k_s^{D_i})[X]} \times \left\{\exp\left[\sum_{i=1}^{n}(k_{u_i} + k_{c_i}[X])l/v_A + (k_s^A - k_s^{D_i})[X]l/v_A\right] - 1\right\} \quad (2)$$

in eq 3, where $a_{1,i} = k_{u_i}l/v_A$, $a_{2,i} = k_{c_i}/v_A$, $b_1 = \Sigma_{i=1}^{n}$

$$\frac{[D_i]}{[A]} = \frac{a_{1,i} + a_{2,i}[X]}{b_1 + b_{2,i}[X]}[e^{b_1 + b_{2,i}[X]} - 1] \quad (3)$$

$k_{u_i}l/v_A$, and $b_{2,i} = [\Sigma_{i=1}^{n} k_{c_i} + (k_s^A - k_s^{D_i})l/v_A$, which can be expanded as shown in eq 4, and which

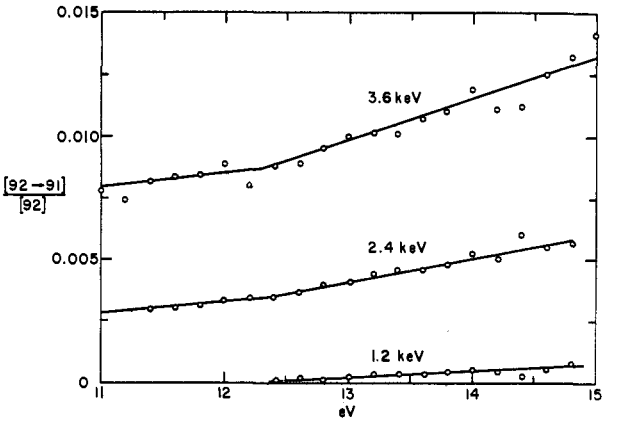

Figure 2. Relative abundance of the $C_7H_7^+$ ions produced by collision of $C_7H_8^+$ from toluene with Ar at 1×10^{-4} Torr as a function of the electron energy producing the $C_7H_8^+$ ions and of the ion accelerating potential.

(23) M. Vogler and W. Seibt, *Z. Phys.*, 210, 337 (1968).

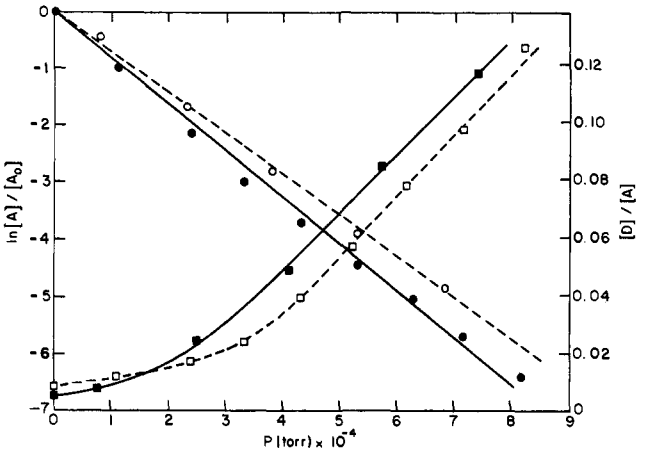

Figure 3. Relative abundances of precursor ions (circles, left ordinate scale) and total product ions (squares, right ordinate scale) as a function of pressure from the collision of (○, □) $C_3H_7^+$ from 2-methylpentane with Ar and (●, ■) $C_2H_5O^+$ from 1-propanol with helium.

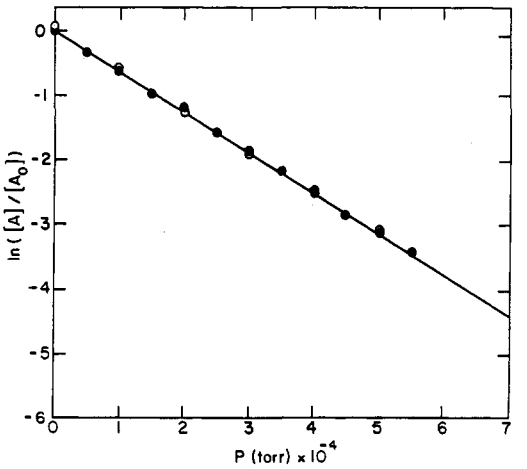

Figure 4. Relative abundances of precursor molecular ions as a function of Ar pressure of (○) anisole and (●) acetophenone.

$$\frac{[D_i]}{[A]} = (a_{1,i} + a_{2,i}[X]) \times \left[1 + \frac{b_1 + b_{2,i}[X]}{2} + \frac{(b_1 + b_{2,i}[X])^2}{6} + \ldots + \frac{(b_1 + b_{2,i}[X])^n}{(n+1)!} + \ldots\right] \quad (4)$$

predicts an initial linear relationship between $[D_i]/[A]$ and [X] which becomes nonlinear at higher collision gas pressures as observed.

This relationship was tested with a detailed study of $[D_i]/[A]$ for five of the transitions from the molecular ion of anisole (Figure 5). The data were measured on the RMH-2, for which not more than a few per cent of the collisions should take place in the ion path outside of the drift region; in addition the high ratio of the collision path length (60 cm) to the ion entrance and exit slit width (0.3 mm) should mainly limit the product ions collected to those of interactions of nearly zero scattering angle. (Measurements of the same anisole transitions on the RMU-7 gave results which were qualitatively very similar.) The lines of Figure 5 were calculated from a nonlinear least-squares fit

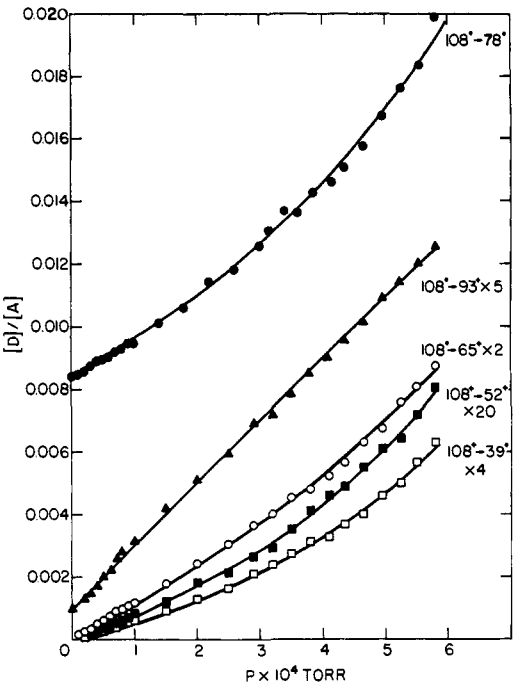

Figure 5. Relative abundances of product ions from the collisional activation of anisole molecular ions as a function of Ar pressure (determined on the RMH-2): (●) $C_6H_6^+$, (▲) $C_6H_5O^+$, (○) $C_5H_5^+$, (■) $C_4H_4^+$, (□) $C_3H_3^+$.

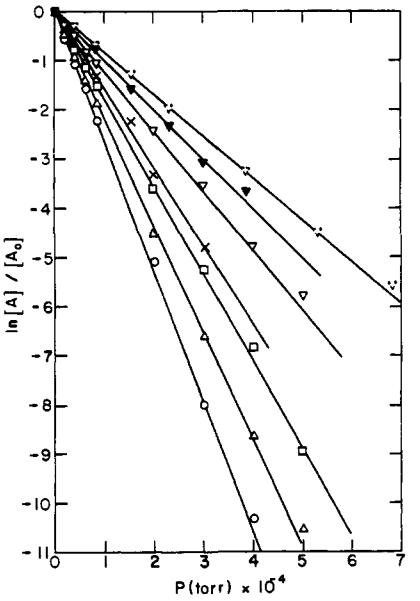

Figure 6. Relative abundances of various ions from acetophenone as a function of Ar pressure in the second field-free drift region of the reversed geometry RMU-7,[7] ion accelerating (IA) potential = 3.9 kV: (○) *m/e* 120, (△) *m/e* 105, (×) *m/e* 105 originating by metastable decomposition of *m/e* 120 in the first drift region; (□) *m/e* 77, (▽) *m/e* 43, (▼) *m/e* 43, He as target gas; (▽) *m/e* 43, He as target gas, IA = 2.5 kV. The data in Figure 6 were taken at one time, as the slopes are quite sensitive to instrument conditions.

of the last equation in which the parameters $a_{1,i}$ and b_1 were obtained from unimolecular metastable intensities and $a_{2,i}$ and $b_{2,i}$ were treated as adjustable parameters. The agreement is within experimental error, although there may be other small effects which could also contribute to the nonlinearity. These include multiple scattering in the collision region, and uni-

molecular and collision processes occurring at points in the instrument ion path outside the collision region. The kinetic treatment has not considered the contribution to the abundance of secondary product ions through secondary collisional formation from primary product ions, *e.g.*

$$108\cdot^{+} \xrightarrow{\text{collision}} 93^{+} \xrightarrow{\text{collision}} 65^{+}$$

The fact that the agreement with theory of the experimental data for the secondary product ions is comparable to that for the primary ions cannot, however, be taken as evidence that such secondary collisional formation is unimportant at high pressures. An additional possible contribution to the nonlinearity of these plots is photon emission from a collisionally excited precursor ion competing with its decomposition.[2b]

Scattering Corrections. To study the effect of ion mass, ion kinetic energy, and target gas on k_s^A, the slopes of plots of ln [A]/[A$_0$] *vs.* pressure were determined for decompositions occurring in the drift region between the magnetic and electrostatic sectors (reversed geometry)[7] using precursor ions generated in the ion source (Figure 6). Relative scattering cross-sections (k_s^A, approximated by the relative slope) were found to be nearly proportional to (mass)$^{2/3}$ at constant kinetic energy for ions from acetophenone (Figure 6) and 1-propanol (not shown) suggesting that scattering is largely determined by ion geometry. Precursor ions produced by metastable decomposition in the first field-free drift region of the reversed geometry RMU-7 appear to give much smaller k_s values than predicted; this is probably due to a contribution from collisionally activated ion decompositions in the first drift region accompanying the pressure increase in the second drift region.

The effect of ion kinetic energy, KE, was determined by changing the ion accelerating potential (Figure 4 plus data not shown[2b]) yielding the relationships $k_s \sim \mathrm{KE}^{-0.19}$ and thus $k_s \sim v^{-0.38}$, where v is the ion velocity. If v is kept constant instead of KE, this effect will give increased scattering for the lighter ions, so that the overall effect under this restriction will be $k_s \sim (\mathrm{mass})^{0.5}$.

In subtracting the contribution of unimolecular metastable dissociation products, $[D_i]_{uni}$, from the abundance of the collisional activation product ions, a correction must be made for the fact that D_i and A ions are scattered with different cross-sections. Any D_i ion formed in the field-free drift region will have the same velocity as its precursor ion and the relative scattering cross-sections, $k_{s'}$, as determined from the slope of ln [A] *vs.* [X] will be related by $k_{s'}^{D_i}/k_{s'}^{A} = (m_{D_i}/m_A)^{0.5}$, where m_{D_i} and m_A are the masses of D_i and A. Assuming D_i ions are formed throughout the drift region by unimolecular decomposition of A and that both D_i and A are scattered according to their respective cross-sections gives $d[A]/dt = k_s^A[A][X] - \Sigma_{i=1}^{n} k_{u_i}[A]$ and $d[D_i]_{uni}/dt = k_{u_i}[A] - k_s^{D_i}[D_i]_{uni}[X]$. Integrating these equations over the drift region gives

$$\frac{[D_i]_{uni}}{[A]} = \frac{[D_{i,0}]_{uni}}{[A_0]}\frac{1}{Q}[e^{Q} - 1]$$

where $Q = [1 - (m_{D_i}/m_A)^{0.5}] \ln [A_0]/[A] + (m_{D_i}/m_A)^{0.5}$. $[D_{i,0}]_{uni}/[A_0]$ and $[D_{i,0}]_{uni}$ is the unimolecular metastable intensity in the absence of the collision gas. The correction factors for unimolecular metastable contributions for the experimental condition [A]/[A$_0$] = 10% are given in Figure 7. Application of these correction factors, as shown in Table I, seldom makes a significant difference as most unimolecular metastables usually involve a small loss of mass.

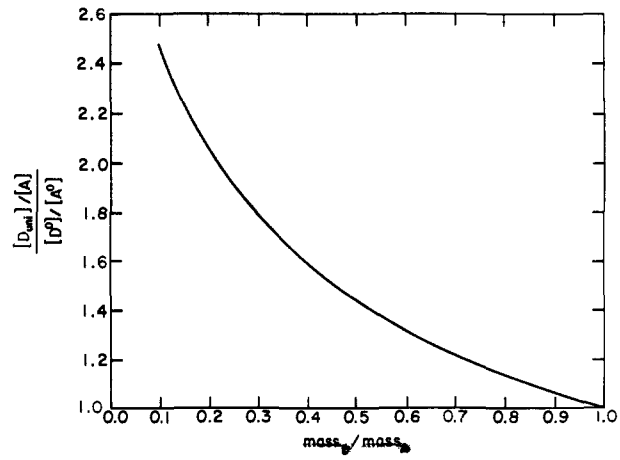

Figure 7. Effect of mass$_D$/mass$_A$ on the relative transmission probability for a product ion D caused by a pressure increase giving [A]/[A$_0$] = 10%.

Effect of the Internal Energy of the Precursor Ion on Its CA Spectrum. The effect of electron energy on log [D]/[A] was studied for 20 different molecular ions of a variety of structures;[18] representative examples are shown in Figures 2, 8, and 9. The largest increase in [D]/[A] found in increasing the electron energy from threshold values to 50 eV was a factor of 15; however, in many cases [D]/[A] is virtually independent of electron energy. The product ion abundances *relative to each other* (the "CA spectrum") exhibit even less change with electron energy, as shown by the parallel relationship of the log [D]/[A] plots of many of the ions to each other. As a rule the product ions showing the largest variation in relative abundance are those of lowest appearance potential.

If the precursor ion is a fragment ion, its internal energy can be decreased by increasing the number of vibrational degrees of freedom (DOF) in the neutral lost in its formation.[4,24] This is illustrated in Figure 10 for the $CH_3C(OH)CH_2\cdot^{+}$ ions produced by single rearrangement from 2-alkanones, and by double rearrangement from 4- and 5-alkanones; the proportion of 58$^+$ ions formed with sufficient energy to undergo the metastable decomposition 58$^+$ → 43$^+$ decreases with increasing number of DOF in the molecular ion producing 58$^+$.[1] The process 58$^+$ → 43$^+$ is the one which yields the most abundant unimolecular metastable; thus, it should also be the reaction in the CA spectrum of these ions whose cross-section is the most dependent on precursor ion internal energy. Figure 10 shows not only that this effect is relatively small in comparison to that for the unimolecular metastables, but that the log cross-section is approximately correlated by 1/DOF in the same manner.

To obtain evidence on the distribution of energy values of the precursor ions immediately after collision, P(E)$_{ac}$, their product ion abundances were com-

(24) F. W. McLafferty and W. T. Pike, *J. Amer. Chem. Soc.*, **89**, 5951 (1967).

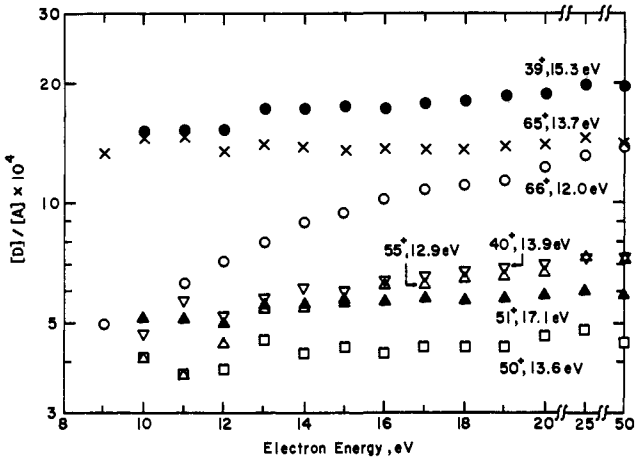

Figure 8. Variation of the relative collisional product ion abundances with ionizing electron energy for phenol. Values of *m/e* and appearance potential of each ion are shown.

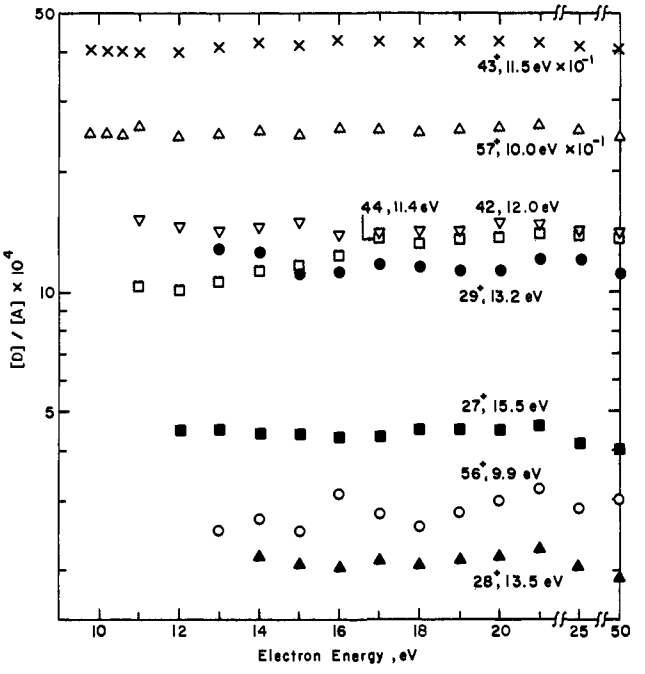

Figure 9. Variation of the relative collisional product ion abundances with ionizing electron energy for 2-butanone. Values of *m/e* and appearance potential of each ion are shown.

pared to those arising from ions of the same structure produced by electron impact. Thus, a difference in the abundance of a particular product ion in the CA *vs.* the EI spectrum should be indicative of a difference in the respective P(E) functions, $P(E)_{ac}$ and $P(E)_{ei}$, for the precursor ion at the energy required to produce that particular product ion. The MI, EI, and CA spectra of additional compounds are compared in Table III with the energy requirements of the product ions. The approximate average energies of the molecular ions involved in the formation of each fragment ion were estimated from breakdown curves derived from charge exchange data; unfortunately, few studies of this type have been made, especially for larger molecules. These energies were also estimated by dividing the total area under the $P(E)_{ei}$ curve (approximated[18] from the photoelectron spectrum convoluted with

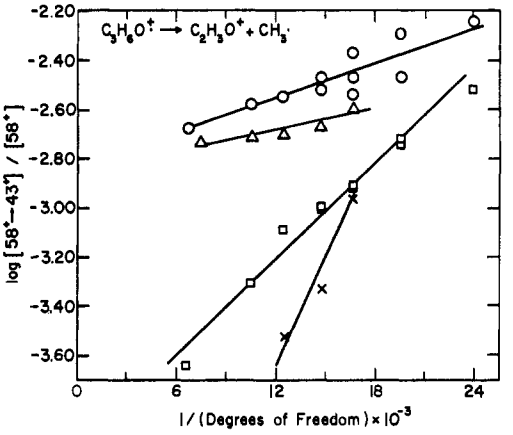

Figure 10. Relative abundances of the $58^+ \rightarrow 43^+$ transition from $C_3H_6O^+$ ions arising from rearrangements in alkanone mass spectra: (□ and ○) single rearrangement, and (× and △) double rearrangement, for unimolecular metastable and collisional activations (Ar, 2.5×10^{-4} Torr) spectra, respectively.

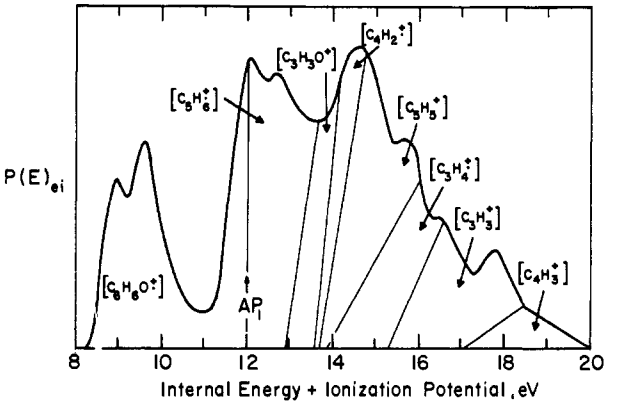

Figure 11. The distribution of internal energy values for phenol molecular ions produced by electron impact divided into arbitrary areas indicating the approximate energies of ions leading to the product ions of the EI spectrum.

the thermal energy)[25] according to the observed EI product ion abundances and appearance potentials (AP). Using $P(E)_{ei}$ of phenol molecular ions as an example (Figure 11), the $C_5H_6^+$ ions will be formed from $C_6H_5OH\cdot^+$ only above their AP value of 12.0 eV. To account for the $C_5H_6^+$ abundance, part of these ions must come from molecular ions produced above 12.9 eV, the AP of $C_3H_3O^+$; the corresponding area in the P(E) curve is divided to reflect the increasing competition for formation of $C_3H_3O^+$ at the expense of $C_5H_6^+$ with increasing energy. Areas for the higher energy ions are assigned in a similar manner, and the average precursor ion energies leading to each daughter are estimated graphically. For 1-propanol the average energies obtained by this method were substantially lower than those from charge exchange data;[26] however, the resulting $P(E)_{ac}$ were quite similar. The $P(E)_{ac}$ function is derived by modifying the $P(E)_{ei}$ function at the average energy of each particular product ion according to the ratio of its abundances in the CA and EI spectra. Examples of the resulting $P(E)_{ac}$ functions are shown in Figures 12 and 13 for colli-

(25) F. W. McLafferty, T. Wachs, C. Lifshitz, G. Innorta, and P. Irving, *J. Amer. Chem. Soc.*, **92**, 6867 (1970).
(26) E. Petterson, *Ark. Fys.*, **25**, 181 (1963).

Table III. Metastable Ion (MI), Collisional Activation (CA), and Electron Impact (EI) Spectra

m/e	AP − IP, eV	Av energy, eV	Spectra MI	CA	EI
		Benzene[a]			
76	4.7	5.2	11	9	7
77	4.7	5.2	87	49	19
52	5.4	5.9	1.4	11	22
39	5.7	7.1	0.8	13	14
50	7.2	8.8	<0.5	6	18
51	8.4	10.8	<0.5	13	21
		Phenol[a]			
66	3.8	4.4	90	19	25
55	4.7	5.3	5	10	8
50	5.4	5.8	<0.5	6	6
65	5.5	6.6	4	18	20
40	5.7	6.9	<0.5	10	12
39	7.1	8.4	<0.5	28	25
51	8.9	10.2	<0.5	8	5
		2-Butanone[a]			
56	0.4	0.6	1	0.4	0.1
57	0.6	1.0	51	35	3
43	1.9	3.8	47	58	63
42	2.4	4.2	<0.5	2	3
29	3.6	6.2	<0.5	2	15
28	3.9	6.5	<0.5	0.3	2
27	5.9	8.2	<0.5	0.6	13
		Acetone[a]			
42	1.3	1.7	88	9	6
43	1.5	4.4	10	86	80
29	3.9	6.2	2	3	3
39	3.9	6.2	<0.2	0.6	3
27	6.4	7.8	<0.2	0.9	0.9
26	6.5	8.9	<0.2	0.5	4
		Propane[b]			
43	0.3	2[c]	99	42	12
28	0.5	5	0.6	26	22
29	0.7	3	<0.1	17	37
42	1.1	5	0.7	1	2
41	2.6	7	<0.1	3	6
27	2.9	8	<0.1	8	12
26	3.6	>9	<0.1	2	2
39	6.0	>11	<0.1	1	7
		Ethanol[b]			
45	0.2	1.5[d]	99	69	24
31	0.7	4.0	<0.2	23	49
29	2.0	8.5	0.5	3	7
27	2.0	8.0	<0.2	2	8
30	2.3	8.5	<0.2	1	3
19	2.5	6.5	<0.2	0.7	2
43	3.0	9.0	<0.2	1	5

[a] Electron energy for all spectra 50 eV; ion abundances based on total fragment ion abundance = 100. Using helium as the target gas with no correction for multiplier response. [b] Using argon at 2.0×10^{-4} Torr as the target gas. [c] W. A. Chupka and J. Berkowitz, *J. Chem. Phys.*, **47**, 2921 (1967); E. Petterson and E. Lindholm, *Ark. Fys.*, **24**, 49 (1962). [d] H. von Koch and E. Lindholm, *ibid.*, **19**, 123 (1961).

sional activation of molecular ions produced at several electron energies.[18]

Factors Affecting $P(E)_{ac}$. Although changing the P(E) of the precursor ion sometimes increases the *overall* cross-section for collisional activation substantially, this has a surprisingly small effect on the *relative* product ion abundances for all but the lowest energy reactions.

A possible explanation is that there is a relatively high cross-section for vibrational excitation to add only a small amount of internal energy. Such excitation would thus lead to only those reactions of lowest appearance potentials, and lowering the ionizing electron

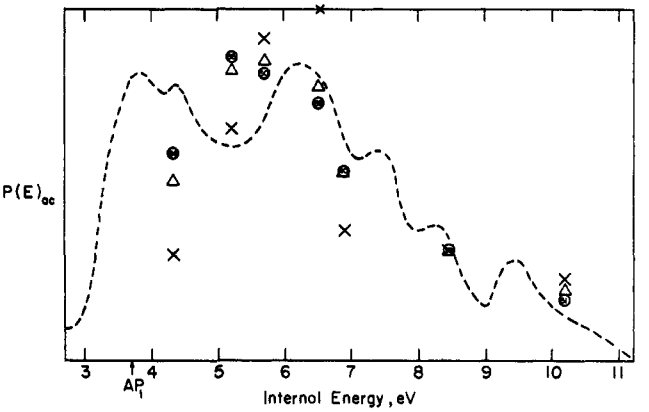

Figure 12. Estimated $P(E)_{ac}$ function for phenol molecular ions at electron energies of (○) 50 eV, (△) 20 eV, and (×) 11 eV. Figures within the circles are the masses of the product ions utilized (see text). Dotted line is the estimated $P(E)_{el}$ function.

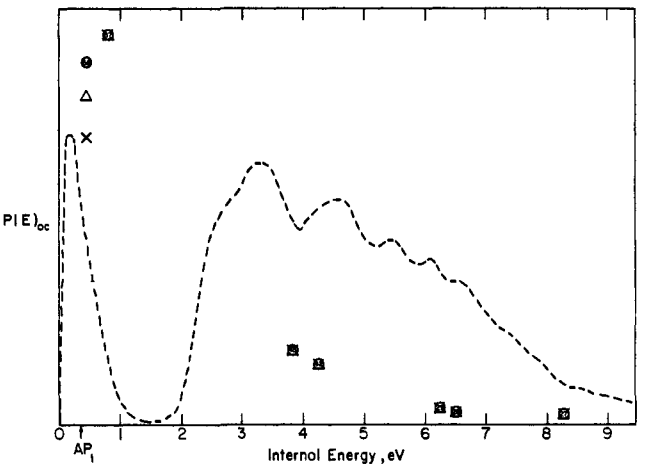

Figure 13. Estimated $P(E)_{ac}$ function for 2-butanone molecular ions at electron energies of (○) 50 eV, (△) 20 eV, and (×) 13 eV. See the legend of Figure 12.

energy below the lowest AP should eliminate precursor ions with sufficient internal energy to undergo decomposition after vibrational excitation. We have observed this in a variety of cases;[18] for example, the slope of the cross-section $[92\cdot^+ \rightarrow 91^+]/[92\cdot^+]$ *vs.* the electron energy used in forming $92\cdot^+$ from toluene (Figure 2) shows a marked increase near AP ($92\cdot^+ \rightarrow 91^+$). This slope change is evident even at 1.2-keV ion accelerating potential at which the cross-section for electronic excitation[27] is severely reduced, consistent with a separate excitation mechanism of relatively high cross-section at low ion kinetic energies.[28] This suggests that even higher ion accelerating voltages should give CA spectra whose relative abundances are even less dependent on precursor ion energy. However, CA spectra omitting the ions from the lowest

(27) Electronic excitation of cations can be caused by photons: R. C. Dunbar, *J. Amer. Chem. Soc.*, **93**, 4354 (1971), has recently shown[28] that the energy onset for photodissociation is determined not only by the thermochemical threshold for the process but also by the energy of the first excited state of the ion.

(28) Durup and coworkers[16] noted a similar slope increase for the collision-induced dissociation $C_2H_2^+ \rightarrow C_2H^+$, which is due to a predissociation process in which the collision causes the ion to undergo a radiationless transition to a dissociative state of the same energy. However, the probability of such isolated energy states should be very low for ions such as these with a substantial number of degrees of freedom.

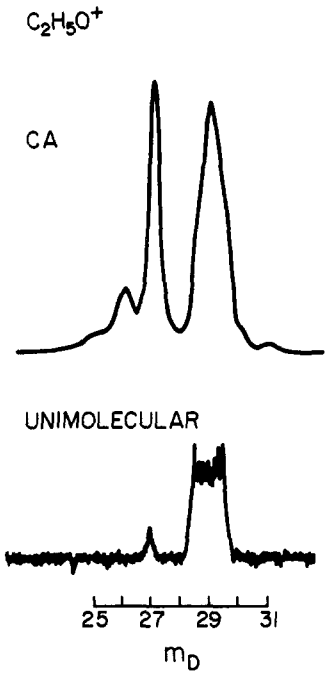

Figure 14. Peaks resulting from the unimolecular metastable (lower trace) and collisional excitation (upper trace) decomposition of $C_2H_5O^+$ ions from 1-propanol in the field-free drift region between the magnetic and electrostatic sectors (reversed geometry)[7] to yield CHO^+.

energy process should provide a specific characteristic of the precursor ion structure;[2a,14] this application will be discussed in a subsequent paper.

The $P(E)_{ac}$ functions of the aromatic compounds show a close general resemblance to the $P(E)_{ei}$ functions of the corresponding ions formed by electron impact, in contrast to those of the aliphatic compounds. For example, benzene and phenol, whose $P(E)_{ei}$ functions have relatively low probabilities at the lower end of the energy range studied, show similar behavior in their $P(E)_{ac}$ functions, while nitrobenzene and benzonitrile show similar high probabilities in the low range of the $P(E)_{ac}$ and $P(E)_{ei}$ functions. These similarities may be due to the fact that the removal of an electron from an aromatic compound causes a relatively small change in molecular configuration, much smaller than that caused in an aliphatic compound. The aromatic molecular ions in general show a much higher transition probability in $P(E)_{ac}$ at higher energies than do the aliphatic ions, even though the corresponding $P(E)_{ei}$ do not.

Even in the low energy region 2-butanone exhibits a striking difference in its $P(E)_{ei}$ and $P(E)_{ac}$ functions. Apparently it is the low probability in the $P(E)_{ei}$ curve at low energies that is the most important cause of the low abundance of the stable $C_2H_5CO^+$ ion, rather than an unfavorable k(E) function; both the unimolecular metastable decomposition and the CA spectrum give abundant $C_2H_5CO^+$ ions. In 2-hexanone (Table I) the corresponding lowest energy process, $100^+ \rightarrow 85^+$, is also far more abundant in the CA spectrum than in the EI spectrum. The spectrum of 2-hexanone-*1,1,1,-3,3,-d*$_5$ shows that this is actually due to two processes involving the loss of CH_3 as well as CD_3;[29] the former is the lower energy process (AP = 9.4 and 10.2, respectively). Although 75% of the methyl-loss product ions in the EI spectrum are found as $(M - CD_3)^+$ in the labeled compound, only 2 and 3% are found thus in the unimolecular metastable spectrum and the CA spectrum (5×10^{-4} Torr of Ar), respectively. Again, this is consistent with a low probability in the corresponding energy region of the $P(E)_{ei}$ function. In many cases, the *product* ions formed by electron impact must also have a relatively narrow range of internal energies. Thus, collisional activation of both molecular and fragment ions could provide a way to produce additional decomposition pathways of either lower or higher energy requirements. As a further consequence of this, the CA spectra of EI molecular and fragment ions from an unknown molecule might provide structural information in addition to that in the EI spectrum. For example, in 2-butanone (Table III) and 2-hexanone (Table I) the CA spectra not only show more abundant large acylium ions than do the EI spectra, but the hydrocarbon ions (27^+, 29^+ and 29^+, 57^+, respectively) are substantially reduced. The structures of odd-electron fragment ions in the EI spectrum of an unknown molecule should be determinable in particular cases by comparison of their CA spectra with those of known molecular ions. Our preliminary studies indicate that structural information concerning even-electron as well as odd-electron ions can be gained from correlations of CA spectra.

Peak Shapes in CA Spectra. Collisionally activated ions formed farthest from the drift region exit will have the highest probability for collisional scattering. This is evident in the peak shapes of ions resulting from decompositions accompanied by the release of kinetic energy,[30] the so-called "*flat-top metastables.*" Figure 14 shows the $45^+ \rightarrow 29^+$ transition from 1-propanol which is known to be accompanied by the release of 0.5 eV of energy;[6] although the unimolecular and collision-induced transitions have very different shapes, they exhibit the same peak widths, and thus involve the same energy release. The central mass region of the peaks is mainly due to ions which have undergone the smallest displacement from the true mass, and have therefore traveled the smallest distance; the proportion of these is substantially increased in the CA peak. This is consistent with opposing effects in CA and MI spectra; there should be decreased scattering losses for ions formed by CA closer to the drift region exit, while there should be an approximately exponential decrease in the probability of unimolecular decompositions with increased travel through the drift region. This change in shape led to our erroneous preliminary conclusion[2a] that much less energy was released when this transition was collisionally induced, which was in contrast to our earlier observation using a different experimental method that the $C_3H_7^+ \rightarrow C_3H_5^+$ transition involved the same energy release for MI and CA spectra.[14] Peak shapes should thus be an additional useful characteristic of CA spectra. As will be discussed more fully in a subsequent paper, the mass position of peaks in the CA spectrum is shifted by an amount equivalent to the kinetic energy, which is

(29) F. W. McLafferty, D. J. McAdoo, and J. S. Smith, *J. Amer. Chem. Soc.*, **91**, 5400 (1969).

(30) J. H. Beynon, R. A. Saunders, and A. E. Williams, *Z. Naturforsch. A*, 20, 180 (1965); J. H. Beynon, M. Bertrand, E. G. Jones, and R. G. Cooks, *J. Chem. Soc., Chem. Commum.*, 341 (1972).

converted to internal energy in the collision process.[31] A shift of 0.1 mass unit in the CA spectrum of Figure 14 would require a kinetic energy loss of 0.9 eV. Such shifts become appreciable, however, for processes involving higher activation energies on precursor ions of higher masses (or when using lower accelerating voltages) and appear to be a valuable way to measure the average energy imparted by collision to the precursor ions yielding a particular product ion.

Applications of this technique to the determination of molecular and ion structures and to the elucidation of unimolecular ion reaction mechanisms will be discussed separately.[32] Collisional activation should be especially valuable for ions generated by chemical or field ionization which exhibit a low degree of fragmentation.

Acknowledgments. The authors acknowledge with pleasure helpful discussions with S. H. Bauer, W. A. Chupka, G. A. Fisk, I. Sakai, H. D. R. Schuddemage, T. Wachs, and B. Widom. Helpful criticisms of the referees led to important modifications of the kinetic treatment.

(31) Similar observations have been made independently in studies of the collisional ionization of rare gas ions: T. Ast, J. H. Beynon, and R. G. Cooks, *J. Amer. Chem. Soc.*, **94**, 6611 (1972).

(32) F. W. McLafferty, R. Kornfeld, W. F. Haddon, K. Levsen, I. Sakai, P. F. Bente III, S.-C. Tsai, and H. D. R. Schuddemage, *J. Amer. Chem. Soc.*, in press.

Vacuum Ultraviolet Absorption Spectra of the Chloromethanes

B. R. Russell,*[1a] L. O. Edwards,[1b] and J. W. Raymonda[1c]

Contributions from the Departments of Chemistry, North Texas State University, Denton, Texas 76203, California State University, Hayward, California 94541, and University of Arizona, Tucson, Arizona 85721. *Received September 6, 1972*

Abstract: The vacuum ultraviolet absorption spectra of the chloromethanes and three dichloroalkanes are given with extinction coefficients in the 50,000–90,000-cm^{-1} region. Assignments of most of the Rydberg transitions are made for methyl chloride; several of the lower energy absorptions of the chloromethanes are assigned by analogy of the spectral features. However, the higher energy absorptions cannot be assigned due to intramolecular perturbations and natural diffuseness of the spectra. Attempts to calculate the intramolecular perturbations in terms of the independent systems approach are discussed. By comparison of the oscillator strengths and band maxima for spectra of the chloromethanes, the $\sigma^* \leftarrow \sigma$ transitions are approximately located. The results are also considered in light of some recent photoelectron spectra of the same compounds. Certain analogies are readily seen, but the full relationship between the optical and photoelectron spectra is not completely understood at this time.

The investigation of the electronic spectra of several molecules which differ sequentially by one atom provides clues for assignments as well as suggesting additional molecular spectra to "test" the plausibility of specific assignments. The vacuum ultraviolet spectra of the fluoromethanes, which involve sequential substitution of fluorine into methane, have been reported and assigned in terms of the independent systems model by Edwards and Raymonda.[2] The absorption bands were assigned to the $(\sigma^* \leftarrow \sigma)_{C-H}$ manifold and evidence was presented for postulating considerable Rydberg-on-hydrogen character for the basic $(\sigma^* \leftarrow \sigma)$ transition in C–H. Transitions arising from the fluorine nonbonding electrons and the $(\sigma^* \leftarrow \sigma)_{C-F}$ manifold are not expected in the energy region investigated. Additional absorption bands have been reported[3] for these fluorine-substituted molecules in a higher energy region. An alternate interpretation,[4] which criticizes the independent systems model, of the fluoromethane spectra in terms of a molecular orbital description has been presented where the absorption bands were assigned as pure Rydberg transitions. That interpretation closely parallels the ideas to be presented here for the chloromethanes.

The chlorine-substituted methanes, in addition to the C–H transitions, are expected to have several absorption bands in the 50,000–90,000-cm^{-1} region arising from the nonbonding electrons and possibly the $(\sigma^* \leftarrow \sigma)_{C-Cl}$ transitions.

The vuv spectra of some of the chloromethane molecules have previously been reported separately with varying degrees of experimental detail.[5,6] The spectrum of methyl chloride was initially reported in this region by Price[5] in 1936, and tentative assignments were given according to the theoretical arguments proposed by Mulliken.[7] In 1955 Zobel and Duncan[6] reported the spectra of the remaining members of this group of molecules and suggested assignments for some of the absorption bands. However, the spectra in these earlier studies were given in terms of relative intensities, and absolute oscillator strengths could not be determined.

In this paper the spectra of the four chloromethanes

(1) (a) North Texas State University; (b) California State University; (c) University of Arizona.
(2) L. Edwards and J. W. Raymonda, *J. Amer. Chem. Soc.*, **91**, 5937 (1969).
(3) G. R. Cook and B. K. Ching, *J. Chem. Phys.*, **43**, 1794 (1965).
(4) C. R. Brundle, M. B. Robin, and H. Basch, *ibid.*, **53**, 2196 (1970).
(5) W. C. Price, *ibid.*, **4**, 539 (1936).
(6) C. R. Zobel and A. B. F. Duncan, *J. Amer. Chem. Soc.*, 77, 2611 (1955).
(7) R. S. Mulliken, *Phys. Rev.*, **47**, 413 (1935); **61**, 277 (1942).